Test limitations induced by fault-driven instability of analog circuits

Wojciech Toczek

Chair of Metrology and Electronic Systems, Gdańsk University of Technology, ul.Narutowicza 11/12, 80-952 Gdańsk, Poland, phone +48 58 3471657, fax +48 583472255, e-mail: toczek@pg.gda.pl

A b s t r a c t - The aim of this paper is to estimate the limitations of parametric faults testing in analog circuits result from fault-driven instability. The linear fractional transformation (LFT) and structured singular value (SSV), the analysis methods from robust control theory, are employed to investigate which parameter could lead to instability of a circuit under test (CUT), and to quantify the deviation in component parameter value that will cause instability. The leapfrog filter is studied as CUT. The SSV based analysis procedure is applied to a Simulink model, which is realized as LFT representation of faulty circuit. Numerical results show that leapfrog filter is highly susceptible to lose stability due to faulty RC elements.

I. Introduction

New developments in the analog and mixed-signal electronics and the increasing market demands such as higher quality, lower costs, shorter time-to-market, result in new challenges in the testing area. Usually, testing of analog circuits is done by verifying all circuit specifications. This is called specification-based testing [1]. This requires specialized, expensive test equipment and results in a long production testing time. As an alternative approach, defect-oriented testing (DOT) methods, based on simple input/output measurements, can be used. This is an active research field that offers potential solutions, which are more similar to digital test methods [2]. An in-depth understanding of inherent limitations of defect-oriented testing in linear analog circuits is a crucial need for designers of DOT methods.

Commonly, a few difficulties and limitations on the testability of faults are considered: the inability to detect small-size soft faults due to manufacturing tolerances, a phenomenon of masking where the existence of one fault prevents an otherwise detectable fault from being detected [3], effect of measurement errors and noise, parasitic effects of the test equipment [4]. In cited papers and most another publications devoted to: the design of analog test criteria [5,6], testability analysis [7,8,9], fault modelling and simulation [10,11] it is assumed that the circuit does not become unstable in the presence of faults.

Under more realistic assumptions it is necessary to take under consideration the requirement of stability. Problem is particularly important for multiple-loop feedback filters, so in this paper the representative of this class - the leapfrog filter (LF) is chosen as the circuit under test (CUT). Fault-driven instability prevents the CUT to perform its function and precludes measurements in most test methodologies. It raises the question of how to ascertain what amount of deviation in component parameter value will cause the unstable behaviour of the CUT. The objective of this paper is using structured singular value analysis, method of robust control theory known as μ-analysis, to address the question of test limitations induced by fault-driven instability. The main advantage of μ-analysis is its ability to quantify the effect of physical parameter deviation on a multiple-input-multiple-output model basis.

In the paper, the standard notation is used. R is the set of all real numbers, C is the set of all complex numbers. With respect to a given matrix, $\sigma_1(.)$ denotes the largest singular value, $\rho(.)$ the spectral radius.

II. Methodology

A. Modelling of faulty circuit with the aid of linear fractional transformation

As the first step of stability analysis, the model of CUT with faults in its physical parameters must be designed on a unified linear fractional transformation (LFT) framework [12].

Suppose **G**(s) is a stable, real rational transfer function matrix of a linear time invariant CUT. The idea is to separate what is known from what is unknown in a feedback-like structure. Fault may be modelled as unknown perturbations to the known nominal model. The CUT can be put in the general diagram in Fig.1, where **G** is the transfer matrix, **Δ** is the representation of parametric faults (matrix of perturbations of transfer function coefficients caused by parametric faults). The signals **u**, **y**, **w** and **z** are vector quantities. The matrix **G** can be partitioned into four submatrices compatible with the sizes of the signal vectors.

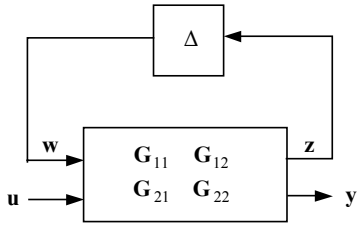

Fig. 1. General LFT framework.

The following relationships can be observed

$$\begin{aligned} \mathbf{w} &= \mathbf{\Delta z} \\ \mathbf{z} &= \mathbf{G_{11} w} + \mathbf{G_{12} u} \\ \mathbf{y} &= \mathbf{G_{21} w} + \mathbf{G_{22} u} \end{aligned} \tag{1}$$

Using the rules of algebra to eliminate **w** and **z** gives the relationship

$$\mathbf{y} = \mathrm{F_u}(\mathbf{G}, \mathbf{\Delta})\mathbf{u}\,, \tag{2}$$

where the closed-loop transfer function

$$\mathrm{F_u}(\mathbf{G}, \Delta) = \mathbf{G}_{22} + \mathbf{G}_{21}\Delta(\mathbf{I} - \mathbf{G}_{11}\Delta)^{-1}\mathbf{G}_{12}\,, \tag{3}$$

provided that the inverse $(\mathbf{I} - \mathbf{G}_{11}\mathbf{\Delta})^{-1}$ exists. The defined above matrix function is known as an upper linear fractional transformation, because the feedback part of the structure is above the matrix **G**. A useful interpretation of an LFT is that it has a nominal mapping, $\mathbf{G_{22}}$, and is perturbed by **Δ**, while $\mathbf{G_{12}}, \mathbf{G_{21}}, \text{and } \mathbf{G}_{11}$ reflect a prior knowledge as to how the fault affects the nominal map, $\mathbf{G_{22}}$ [12].

B. The structured singular value

Perturbation matrix **Δ** is referred to as a structured perturbation if it is restricted to the set $\overline{\mathbf{\Delta}}$. Define the structured perturbations $\overline{\mathbf{\Delta}} \subset \mathrm{C}^{n\times n}$ as

$$\overline{\mathbf{\Delta}} = \left\{ \mathrm{diag}\left[\delta_1 \mathbf{I}_{r1}, ..., \delta_s \mathbf{I}_{rs}, \mathbf{\Delta}_1, ..., \mathbf{\Delta}_F\right] : \delta_i \in \mathrm{C},\ \mathbf{\Delta}_j \in \mathrm{C}^{m_j \times m_j} \right\} \tag{4}$$

where: S represents the number of single or repeated scalar diagonal elements, δ_i is either real or complex and **I** is the identity matrix, F represents the number of full complex blocks, positive integers $r_1, ..., r_S;\ m_1, ..., m_F$ are their dimensions, the *i*-th repeated scalar block is $r_i \times r_i$, while the *j*-th full complex block is $m_j \times m_j$. To be used in the μ framework, the variation parameters must be normalized. Each real δ_i is normalized to the interval [-1,1] and complex parameters to the unit circle.

Let $\mathbf{M} \in \mathrm{C}^{n\times n}$ be a given matrix. The structured singular value (SSV) μ of the matrix **M** with respect to the set $\overline{\mathbf{\Delta}}$ of allowable perturbations with the specified structure (4) is defined as

$$\mu_{\overline{\Delta}}(\mathbf{M}) = \begin{cases} 0, & \text{if } \det(\mathbf{I} - \mathbf{M\Delta}) \neq 0; \\ (\inf\{\sigma_1(\mathbf{\Delta}) \mid \det(\mathbf{I} - \mathbf{M\Delta}) = 0\})^{-1}, & \text{otherwise.} \end{cases} \tag{5}$$

The structured singular value μ has the following property [12]

$$\rho(\mathbf{M}) \le \mu_{\overline{\Delta}}(\mathbf{M}) \le \sigma_1(\mathbf{M})\,. \tag{6}$$

These bounds are not sufficient for practical purposes because the gap between ρ and σ_1 can be arbitrarily large. However, the bounds can be refined by using transformations on **M** that do not affect $\mu_\Delta(\mathbf{M})$, but do affect ρ and σ_1.

$$\max_{\mathbf{U}\in\mathbf{U}} \rho(\mathbf{UM}) \le \mu_{\underline{\Delta}}(\mathbf{M}) \le \inf_{\mathbf{D}\in\mathbf{D}} \sigma_1(\mathbf{DMD}^{-1}) \tag{7}$$

where: $\mathbf{U}$ and $\mathbf{D}$ are two subsets of $C^{n\times n}$, and any $\mathbf{U}\in\mathbf{U}$, $\mathbf{D}\in\mathbf{D}$

$$\mathbf{U} = \{\mathbf{U}\in\overline{\mathbf{\Delta}} : \mathbf{UU}^* = \mathbf{I}_n\},$$

$$\mathbf{D} = \{\mathrm{diag}[\mathbf{D}_1,...,\mathbf{D}_S, d_1\mathbf{I}_{m1},...,d_F\mathbf{I}_{mF}] : \mathbf{D}_i \in C^{r_i\times r_i}, \mathbf{D}_i = \mathbf{D}_i^* > 0, d_j \in R, d_j > 0\}.$$

It has been shown [12] that $\max_{\mathbf{U}\in\mathbf{U}} \rho(\mathbf{UM}) = \mu_{\underline{\Delta}}(\mathbf{M})$ always holds. However, the quantity $\rho(\mathbf{UM})$ can have multiple local maxima that are not global. Thus local search cannot be guaranteed to obtain μ, but can only yield a lower bound. For reliable use of the μ-analysis, it is essential to have upper and lower bounds. The upper bound can be reformulated as a convex optimisation problem, so the global minimum can be found, but the upper bound is equal to μ only for block structures with $2S+F\le 3$. An implementation of routines to numerically calculate the μ bounds is provided in the μ-Analysis and Synthesis Toolbox of Matlab. Also reliable computational tools are available as the freeware [13].

C. The marginal stability

Marginal stability means that the CUT is on the boundary between stable and unstable behaviour. Circuit is marginally stable when there are unrepeated poles having a real part of zero and no poles with positive real parts.

Theorem [12]. Let $\beta > 0$. The system (Fig. 1) is stable for all $\mathbf{\Delta}\in\overline{\mathbf{\Delta}}$ with $\|\mathbf{\Delta}\|_\infty < \frac{1}{\beta}$ if and only if $\mathbf{G}(s)$ is stable and $\sup_{\omega\in R} \mu_{\underline{\Delta}}(\mathbf{G}(j\omega)) \le \beta$.

Hence, the reciprocal of the structured singular value (μ^{-1}) corresponds to the smallest perturbation matrix $\mathbf{\Delta}$, in the sense of $\sigma_1(\mathbf{\Delta})$, such that will cause a CUT to go marginally stable.

III. Calculation of the stability margins for circuit under test

In this section the limitations induced by fault-driven instability of leapfrog filter, taken from [14] as circuit under test, are studied.

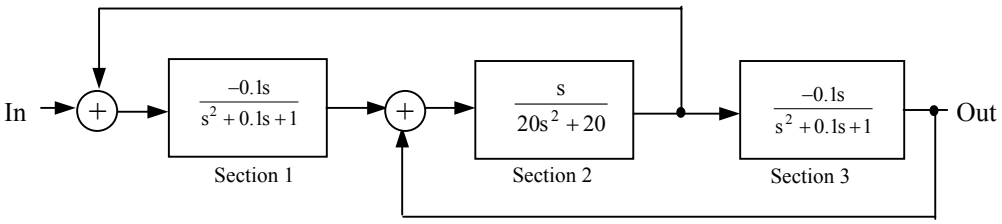

Fig. 2. Overal leapfrog filter realizing the sixth-order Butterworth bandpass function.

The sixth-order Butterworth bandpass function is realized with the application of negative feedback in cascade connection of second–order sections (Fig. 2).

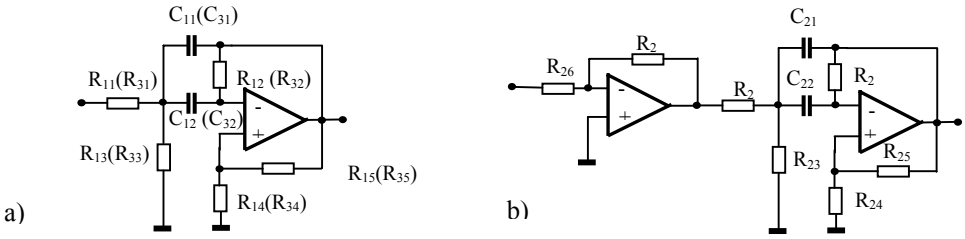

Fig. 3. Realization of filter from Fig. 2 (a) Section 1 and Section 3, (b) Section 2.

Each section is based on single amplifier biquad (SAB) presented in Fig. 3. a.
Assuming that the operational amplifier is ideal, the transfer function of a SAB is as following:

$$T(s) = -\frac{\frac{(1+K)R_3}{RC_2(R_1+R_3)}s}{s^2 + [\frac{1}{R_2}(\frac{1}{C_1}+\frac{1}{C_2}) - K\frac{1}{RC_2}]s + \frac{1}{RR_2C_1C_2}}, \quad \text{where: } K = \frac{R_4}{R_5}, R = \frac{R_1R_3}{R_1+R_3} \tag{8}$$

Normalized component values for the overall filter are given in Table 1.

Table 1. Normalized component values.

SAB	Section 1		Section 2		Section 3	
R_1	R_{11}	10.27	R_{21}	2.082	R_{31}	10.27
R_2	R_{12}	7	R_{22}	7	R_{32}	7
R_3	R_{13}	0.1449	R_{23}	0.1534	R_{33}	0.1449
R_4	R_{14}	0.2	R_{24}	2	R_{34}	0.2
R_5	R_{15}	7.54	R_{25}	49	R_{35}	7.54
R_6	R_{16}	-	R_{26}	1	R_{36}	-
R_7	R_{17}	-	R_{27}	0.1	R_{37}	-
C_1	C_{11}	1	C_{21}	1	C_{31}	1
C_2	C_{12}	1	C_{22}	1	C_{32}	1

Table 2. Pole location of the nominal CUT.

Eigenvalue	Damping	Freq. (rad/s)
-2.40e-2 + 9.57e-1i	2.50e-2	9.58e-1
-2.40e-2 - 9.57e-1i	2.50e-2	9.58e-1
-5.00e-2 + 9.99e-1i	5.00e-2	1.00e+0
-5.00e-2 - 9.99e-1i	5.00e-2	1.00e+0
-2.61e-2 + 1.04e+0i	2.50e-2	1.04e+0
-2.61e-2 - 1.04e+0i	2.50e-2	1.04e+0

The Simulink model of faulty circuit designed in the LFT framework is depicted in Fig. 4. It has hierarchical structure, contained Subsystem 1 that is realization for transfer matrices of the second section of CUT, in which capacitor C_{21} is assumed to be faulty. It is seen from eq. (8) that in the case of faulty capacitor C_{21} second section is affected in two places (two coefficients of the transfer function of the second section depend upon the parameter of faulty capacitor C_{21}). In consequence, Subsystem 1, beside of input and output, has two pairs of additional terminals (1-1 and 2-2) dedicated to realize connections with perturbation matrix **Δ**.

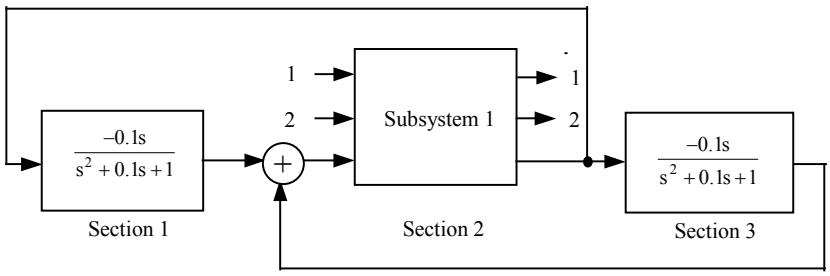

Fig. 4. Simulink model of sixth-order leapfrog filter with faulty capacitor C_{21} in the section 2.

In this way faults are modelled as repeated real scalar elements in **Δ**. This is a serious problem because for pure real perturbation, the computation of lower bound on μ mostly fails. To cope with this difficulties a full complex block is added to regularize the μ problem. This block provides additional small amount of complex uncertainties (5%) that is added to the real fault. Such intervention improves the convergence properties of the algorithm, which computes a lower bound of μ [13]. Results of μ-analysis for 15 single faults are presented in Table 3.

Table 3. Results of μ-analysis for 15 single faults.

	R_{12}	R_{22}	R_{32}	R_{14}	R_{24}	R_{34}	R_{15}	R_{25}	R_{35}	C_{11}	C_{21}	C_{31}	C_{12}	C_{22}	C_{32}
$\underline{\mu}$	1.85	8.79	1.85	1.25	2.90	1.25	2.25	3.89	2.25	0.43	6.01	0.43	1.43	7.01	1.43
$\overline{\mu}$	1.85	8.79	1.85	1.25	2.93	1.25	2.25	3.93	2.25	1.00	6.01	1.00	1.43	7.01	1.43
SM	0.54	0.11	0.54	0.80	0.34	0.80	-0.45	-0.26	-0.45	2.34	0.17	2.34	-0.70	-0.14	-0.70

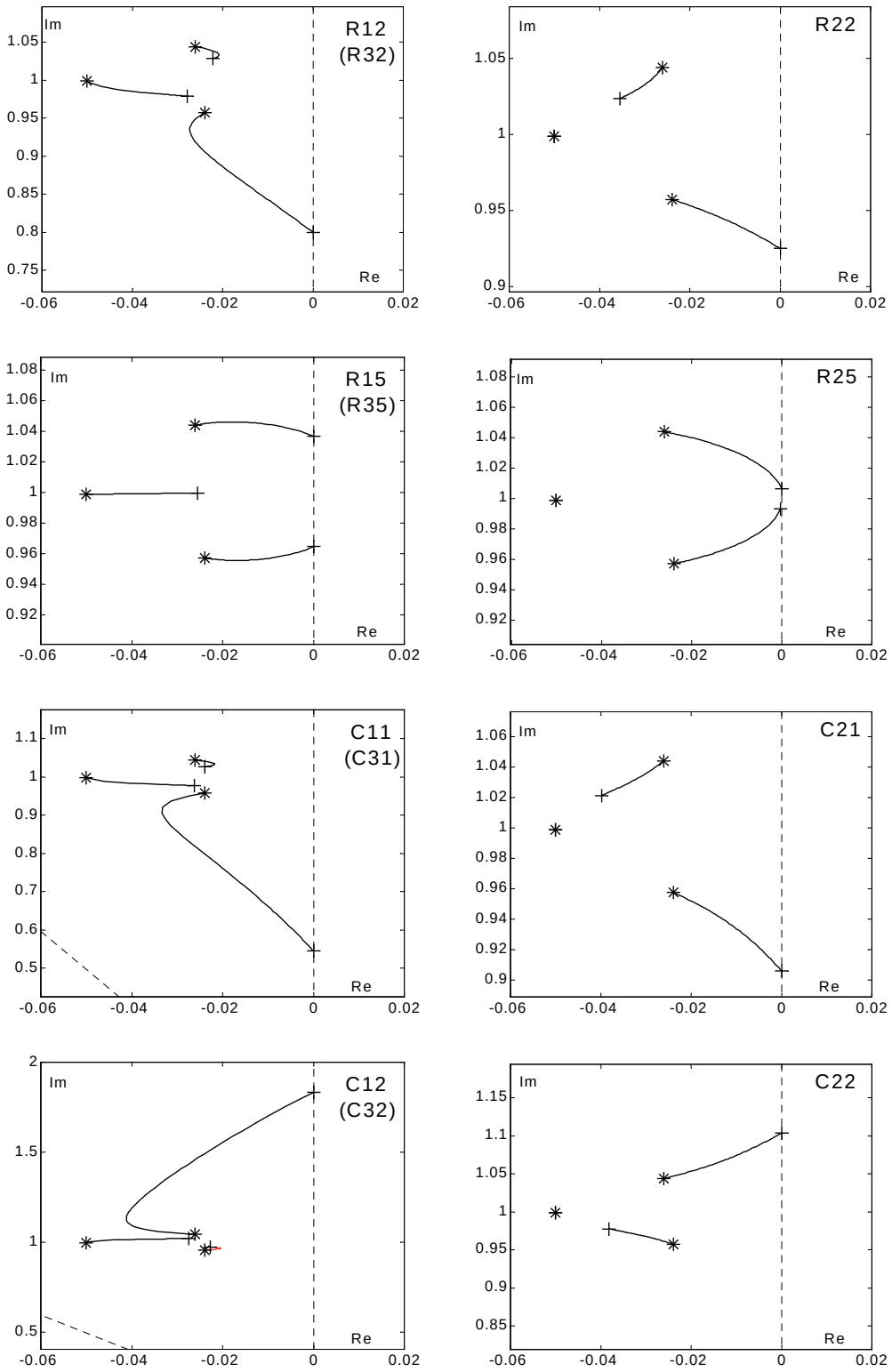

Fig. 5. The zoomed root loci, associated to the smallest perturbation of faulty elements (resistors and capacitors) that leads to marginal stability of circuit under test. Markers (∗) point initial and markers (+) point final positions of the poles.

The second row of Table 3 contains the lower bounds $\underline{\mu}$ of the maximal values of μ over the frequency range 0.1 - 2 rad/s. The upper bounds $\overline{\mu}$ (the third row) assess how well the corresponding lower bound is or validate if it is exact value.

From these results it is possible to predict the smallest perturbations that will cause the CUT to go marginally stable. Stability margins (SM) are equivalent to reciprocals of the structured singular values

1/ $\underline{\mu}$. Stability margins, presented in the last row of Table 3, form hyper-cube in device-level parameter space in which the CUT is stable and can be tested. It is seen that section 2 is highly susceptible to lose stability due to the faulty RC elements. Note that in the face of resistance R_{22} variation greater then 11% circuit will be unstable.

For verification of the results, the root locus method was used. Fig. 5 presents pole movement in the closed-loop model, from nominal locations (Table 2) to final locations due to single faults. The final positions of poles on imaginary axis of the s-plane confirm marginal stability of the CUT for the estimated size of faults. Sections 1 and 3 behave in the same manner - faults affect three pairs of poles, while section 2 manifests different behaviour - faults affect only two pairs of poles. In the case of faulty R_5, (R_{15}, R_{25}, R_{35} in respective sections of filter), two pairs of poles are driven onto the imaginary axis simultaneously.

IV. Conclusions

Fault-driven instability of CUT is the most fundamental limitation of the circuit functionality that has to be taken into account by test designers. It has been shown, on the example of leapfrog filter, that there are faults that will destabilize the CUT. With the aid of tools from the robust control theory the bounds of the device-level parameter space that limit the stability, and in consequence the testability of electronic CUT, have been estimated.

The presented technique of stability analysis can be used to provide a really applicable test design and evaluation, for example to reduce the number of simulations before test. Another application is to use fault-induced instability as the criterion of distinction between soft and hard faults. In marginal stability the CUT produces a bounded response other than the original steady state one. It doesn't perform its function properly, so the fault-induced marginal stability can be classified as the effect of hard fault.

The disadvantage of applying linear method of stability analysis is that some destabilizing phenomena are inherently non-linear in nature and will not be taken into consideration.

References

1. Burns M., Roberts G., W.: *An Introduction to Mixed-Signal IC Test and Measurement*, Oxford University Press, 2001.
2. Huertas J.L.: Test and Design-for-Testability in Mixed-Signal Integrated Circuits, Kluwer, 2004.
3. Savir J., Guo Z.: *Test Limitations of Parametric Faults in Analog Circuits*, IEEE Transactions on Instrumentation and Measurement, vol. 52, No. 5, pp. 1444 -1454, 2003.
4. Iyer M.K., Bushnell M. L.: *Efect of noise on analog circuit testing*, J. Electronic Testing: Theory Application, vol. 15, pp. 11-22, 1999.
5. Lindermeir W., M.Graeb, H.E. Antreich, K. J.:*Analog Testing by Characteristic Observation Inference*, IEEE Transactions on Computer-Aided Design of Integrated Circuits and Systems, vol.18, No 9, pp.1353-1368, 1999.
6. Lindermeir W. M.: *Design of Robust Test Criteria in Analog Testing*, Proc. IEEE Int. Conf. Computer - Aided Design ICCAD'96, Nov. 1996, pp. 604-611.
7. Hemink G.J., Meijer B., W. Kerkhoff, H. G.: *Testability analysis of analog systems*, IEEE Trans. Computer - Aided Design, vol. 9, 1990, pp. 573-583.
8. Heming G.J.:*Testability analysis of analog systems*, IEEE Trans. On Computer-Aided Design, vol. 9, No 6, pp. 573-583, 1999.
9. Slamani M., Kaminska B.: *Fault observability of analog circuits in frequency domain*, IEEE Trans. Circuits Syst. II: Analog and Digital Signal Processing, vol. 43, pp. 134-139, 1996.
10. Perkins A. J., Zwolinski M., Chalk C. D., Wilkins B. R.:*Fault Modeling and Simulation Using VHDL-AMS*, Analog Integrated Circuits and Signal Processing, 16, pp.53-67, 1998.
11. Khouas A., Derieux A.: *Fault Simulation for Analog Circuits Under Parameter Variations*, Journal of Electronic Testing: Theory and Applications, vol.16, pp.269-278, 2000.
12. Zhou K.: *Essentials of robust control*. Prentice-Hall International, Inc., 1998.
13. Ferreres G., Biannic J.M.: *Skew Mu Toolbox*, 2003, software complement to the book by G. Ferreres: *A practical approach to robustness analysis with aeronautical applications*, Kluwer Academia /Plenum Publishers, 1999.
14. Deliyannis T., SunY., Fidler J.K.: *Continuous-Time Active Filter Design*, CRC Press, 1999.